ENDOVASCULAR
AORTIC SURGERY

A computational analysis of different endograft designs for Zone 0 aortic arch repair[†]

Theodorus M. van Bakel[a,b,c,*], Christopher J. Arthurs[d], Joost A. van Herwaarden[c], Frans L. Moll[c], Kim A. Eagle[e], Himanshu J. Patel[f], Santi Trimarchi[b] and C. Alberto Figueroa[a,g]

[a] Department of Surgery, University of Michigan, Ann Arbor, MI, USA
[b] Thoracic Aortic Research Center, Policlinico San Donato IRCCS, University of Milan, San Donato Milanese, Milan, Italy
[c] Department of Vascular Surgery, University Medical Center Utrecht, Utrecht, Netherlands
[d] Division of Imaging Sciences and Biomedical Engineering, King's College London, London, UK
[e] Department of Internal Medicine, University of Michigan, Ann Arbor, MI, USA
[f] Department of Cardiac Surgery, University of Michigan, Ann Arbor, MI, USA
[g] Department of Biomedical Engineering, University of Michigan, Ann Arbor, MI, USA

* Corresponding author. Department of Surgery, University of Michigan, Theodorus van Bakel, 2800 Plymouth Road Building 20-211W, Ann Arbor, MI 48105, USA. Tel: +1-734-5481660; e-mail: vanbakel@med.umich.edu (T.M. van Bakel).

Abstract

OBJECTIVES: Aortic arch repair remains a major surgical challenge. Multiple manufacturers are developing branched endografts for Zone 0 endovascular repair, extending the armamentarium for minimally invasive treatment of aortic arch pathologies. We hypothesize that the design of the Zone 0 endograft has a significant impact on the postoperative haemodynamic performance, particularly in the cervical arteries. The goal of our study was to compare the postoperative haemodynamic performance of different Zone 0 endograft designs.

METHODS: Patient-specific, clinically validated, computational fluid dynamics simulations were performed in a 71-year-old woman with a 6.5-cm saccular aortic arch aneurysm. Additionally, 4 endovascular repair scenarios using different endograft designs were created. Haemodynamic performance was evaluated by calculation of postoperative changes in blood flow and platelet activation potential (PLAP) in the cervical arteries.

RESULTS: Preoperative cervical blood flow and mean PLAP were 1080 ml/min and 151.75, respectively. Cervical blood flow decreased and PLAP increased following endovascular repair in all scenarios. Endografts with 2 antegrade inner branches performed better compared to single-branch endografts. Scenario 3 performed the worst with a decrease in the total cervical blood flow of 4.8%, a decrease in the left hemisphere flow of 6.7% and an increase in the mean PLAP of 74.3%.

CONCLUSIONS: Endograft design has a significant impact on haemodynamic performance following Zone 0 endovascular repair, potentially affecting cerebral blood flow during follow-up. Our results demonstrate the use of computational modelling for virtual testing of therapeutic interventions and underline the need to monitor the long-term outcomes in this cohort of patients.

Keywords: Computational fluid dynamics • Haemodynamics • Thoracic endovascular aortic repair • Branched endograft • Cerebral blood flow

INTRODUCTION

Open surgical repair of aortic arch pathologies remains a major challenge in aortic surgery that requires sternotomy or thoracotomy and cardiopulmonary bypass [1]. Many patients are not considered fit for this invasive procedure due to pre-existing comorbidities [2].

To address this issue, multiple device manufacturers are developing Zone 0 endografts for total endovascular repair of the aortic arch, eliminating the need for open surgical repair [3]. This approach involves deployment of an endograft in the ascending aorta with either 1 or 2 branches that redirect flow to the brachiocephalic trunk (BCT) alone or to the BCT and left common carotid artery (LCCA), in combination with 1 or 2 extra-anatomical bypasses [4]. Different Zone 0 endograft designs have been introduced, with varying number, size and orientation of the branches that redirect flow to the supra-aortic arteries [3].

Early results of Zone 0 endovascular aortic arch repair are promising and encourage the use of these devices, especially in patients with aortic pathologies that would be considered unrepairable otherwise [4, 5]. Stroke remains a significant complication

[†]Presented at the 7th Annual Scientific Meeting of the International Society for Neurovascular Disease, Taormina, Italy, 4 May 2017.

following endovascular repair of the aortic arch [4, 6, 7], with reported incidences up to 11% [4]. Guidewire manipulation and covering of the supra-aortic arteries are procedural factors known to increase stroke risk [5, 7]. Yet, little is known about the impact of the branched endograft design on the risk for cerebrovascular complications. We hypothesize that the design of the Zone 0 endograft has a significant impact on the postoperative haemodynamic performance, particularly in the cervical arteries.

The goal of the present study was to assess and compare the postoperative haemodynamic performance of different Zone 0 endograft designs. Advanced computational fluid dynamics (CFD) tools have been used to support clinical decision-making through calculation of the haemodynamic outcomes of different therapeutic interventions using a 'virtual testing' paradigm [8–10]. The virtual testing paradigm, which has been used in various engineering fields to replace the 'build-and-test' paradigm, uses computational simulations to optimize a proposed design before any physical model is built. We applied these methods in a patient with a saccular aortic arch aneurysm to calculate the cervical blood flow (CBF) and blood shear rates in 4 virtual postoperative scenarios featuring different Zone 0 endograft designs.

METHODS

Approval for this study was obtained from the institutional review board (University of Michigan protocol number HUM00112350), and the need for patient consent was waived.

Patient history

A 71-year-old woman presented with a 6.5-cm isolated saccular aortic arch aneurysm. Her medical history included hypertension, obstructive sleep apnoea, dilated non-ischaemic cardiomyopathy and paroxysmal atrial fibrillation for which a dual-chamber implantable cardioverter defibrillator had been implanted.

Clinical data

Computed tomography angiography was performed using a 64-slice scanner after intravenous injection of 150 ml of iopamidol 76% contrast agent. Ultrasonography examinations of the heart and the cervical arteries were acquired, including measurements of surface area and flow velocity with duplex Doppler ultrasonography, enabling calculation of flow volumes in the cervical arteries. A cardiac catheterization procedure was performed using 80 ml of iopamidol 76% contrast agent, providing information on aortic pressure and cardiac output via the Fick principle [11].

Patient-specific computational modelling

Computational modelling techniques were used to calculate patient-specific haemodynamics based on the physical laws of fluid flows. CFD is a well-established technique that enables calculation of the motion of an incompressible fluid by solving the Navier–Stokes equations. CFD methods have been used profusely in applications such as aerospace and automotive engineering. Over the past decades, CFD methods have also been applied to study haemodynamics in cardiovascular health and disease [12]. Here, a computational model of haemodynamics requires the

definition of: (i) a 3D geometric model of the vessels of interest and (ii) a set of inflow and outflow boundary conditions that represent the flow and pressure conditions of the subject.

For this study, we first produced a validated baseline (preoperative) solution, matching patient-specific clinical measurements on cardiac output, aortic pressure and CBF [10]. Then, the geometry of the preoperative model was modified to construct 4 postoperative scenarios featuring different Zone 0 endograft designs, representing the currently available branched endograft options for total endovascular repair of the aortic arch [3]. All scenarios were run with the same inflow and outflow boundary conditions. Using this 2-step approach, we can quantify haemodynamic alterations induced by the different endograft designs based on the physical laws of fluid dynamics.

The preoperative patient-specific geometric model was built from the computed tomography angiography image data using the validated custom software package CRIMSON [13]. The preoperative model and the 4 endovascular repair scenarios are presented in Fig. 1. A summary of the specifications of the endograft designs is listed in Table 1. All Zone 0 endovascular repair models included an extra-anatomical bypass from the LCCA to the left subclavian artery (8-mm diameter).

Scenario 1 used an endograft with 2 antegrade inner branches of equal diameter positioned side by side, carrying blood flow to the BCT and LCCA. Scenario 2 also featured an endograft with 2 antegrade inner branches; however, the inner branch to the LCCA had a smaller diameter and was positioned oblique behind the inner branch to the BCT. Scenario 3 used an endograft with a single retrograde inner branch carrying flow to the BCT, combined with an extra-anatomical bypass from the right common carotid artery to the LCCA (8-mm diameter). Finally, Scenario 4 used an endograft with a single volcano-shaped branch redirecting flow to the BCT, combined with an extra-anatomical bypass from the right common carotid artery to the LCCA (8-mm diameter).

To solve the blood flow equations, a computational mesh is required. The mesh breaks down the anatomical model into many small elements. The resolution of the mesh must be such that it captures the complex velocity patterns near and around the branches of the device and the vessel walls. Therefore, automatic mesh refinement procedures [14] were used to capture such haemodynamics. Figure 2 presents a cut-through view of the mesh with the total number of elements noted for each model. The models with inner branches (Scenarios 1, 2 and 3) required significantly more elements to produce similar accuracy as the preoperative and Scenario 4 models.

Blood was modelled as a Newtonian fluid with a density of $1060 \, kg/m^3$ and a dynamic viscosity of $0.004 \, Pa \cdot s$. The vessel walls were modelled as rigid. A volumetric flow waveform was imposed at the inflow face of the ascending aorta using echocardiography data, adjusted to match the cardiac output measured during cardiac catheterization via the Fick principle [11]. As outflow boundary conditions, 3-element Windkessel models were specified representing the behaviour of the distal vascular bed at each outlet [15]. A 3-element Windkessel model consists of 3 parameters: a proximal resistor, capacitor and distal resistor. The numerical values of these parameters were tuned to match the clinical measurements from duplex Doppler ultrasonography and cardiac catheterization. The choice for this type of boundary condition was motivated by the fact that in virtual surgical planning, no direct measurements of postoperative flow and pressure are typically available. Furthermore, due to the lack of patient-specific flow measurements at the left and right subclavian
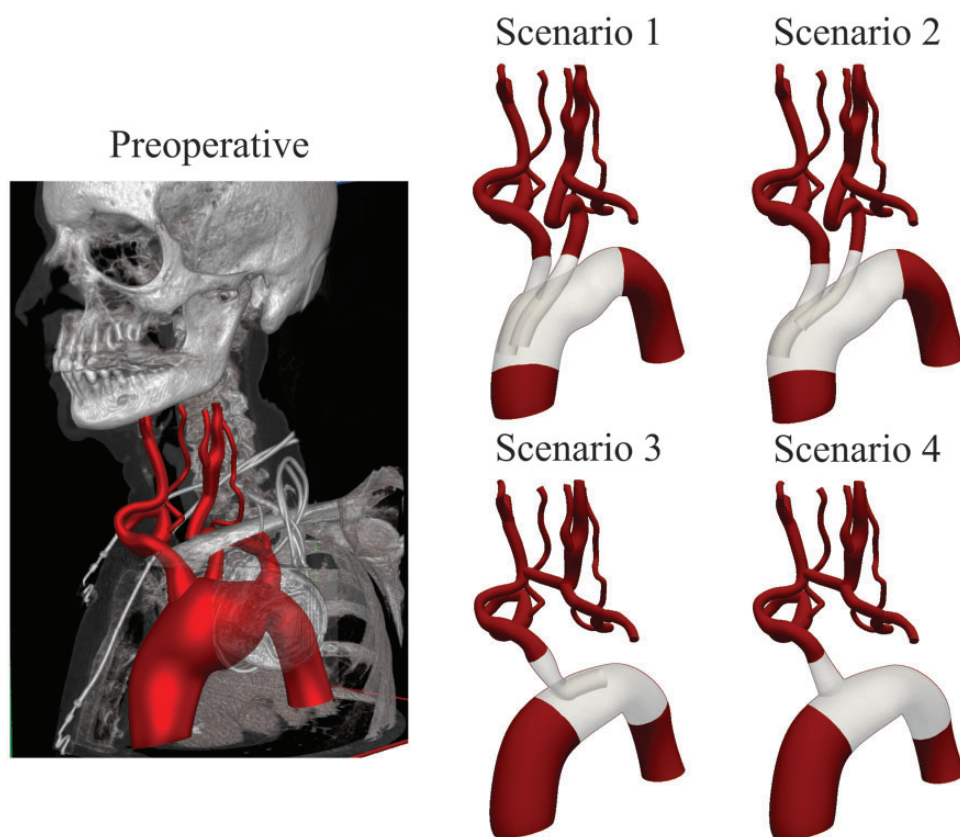
Figure 1: Geometric models of the preoperative situation and 4 endovascular repair scenarios.

Table 1: Specifications of endograft designs

Scenario	Number of branches	Branch orientation	Dimensions of inner branch to BCT (mm)	Dimensions of inner branch to LCCA (mm)
1	2	Antegrade	12 × 44	12 × 40
2	2	Antegrade	12 × 21	8 × 21
3	1	Retrograde	12 × 25	NA
4	1	Cranial	NA	NA

Dimensions of the inner branches are given in diameter × length.
BCT: brachiocephalic trunk; LCCA: left common carotid artery.

arteries, we assigned previously reported flow rates measuring 6% of the cardiac output to each subclavian artery [16]. The numerical values of the Windkessel parameters are reported in Supplementary Material, Table S1.

Computations were performed using the CRIMSON incompressible Navier–Stokes flow solver on 80 cores at the University of Michigan high-performance computing cluster ConFlux. Typical computational time was 24 h per cardiac cycle, varying depending on the number of elements in the mesh.

Particle tracking and platelet activation potential

In addition to quantifying flow and pressure waveforms in the cervical arteries for the different scenarios, we were interested in assessing the risk of thrombus formation relative to the preoperative configuration. It is well known that high blood shear rates lead to platelet activation and can trigger thrombus formation [17, 18]. Therefore, we used a CFD tool called 'particle tracking', which enables tracing the path of thousands of blood particles as they move through the aorta and endograft. We can then calculate a metric known as 'platelet activation potential' (PLAP) [19, 20], which has been recently linked to thrombus formation in thoracic and abdominal aortic flows [8, 20]. The PLAP metric is a dimensionless scalar quantifying accumulated blood shear rate. Using PLAP, the impact of endograft-induced shear distortion can be compared between the different virtual endovascular repair scenarios. In this work, 110 000 particles were injected at the ascending aorta and collected in virtual spheres at the outflows of the supra-aortic arteries (Fig. 3).

RESULTS

### Flow and pressure waveforms in the preoperative model

The preoperative simulation successfully reproduced the clinical data of the patient. Figure 4 presents the computed preoperative flow and pressure waveforms and a comparison between clinical data and computation results at selected locations. All computed flow and pressure values lay within 5% of the clinical data.

Impact of endograft design on cervical blood flow

Table 2 presents the computed mean flow for the preoperative and 4 endovascular repair scenarios. Blood flow to the right
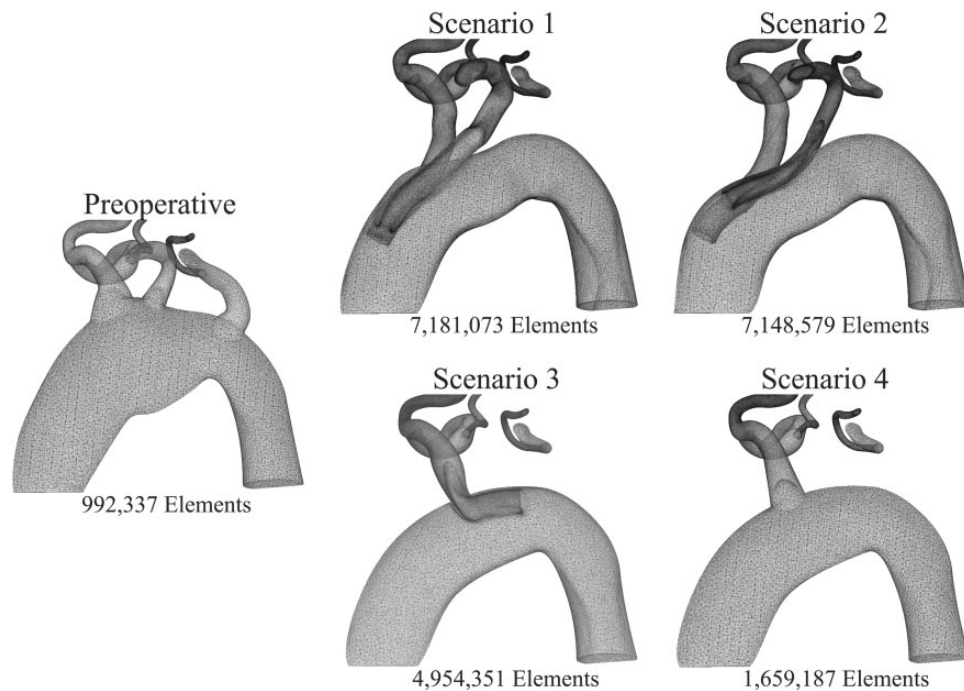
Figure 2: Computational mesh refinement near the supra-aortic arteries in the preoperative anatomy (left) and in the 4 endovascular repair scenarios (right). Mesh refinement is needed to capture complex haemodynamics around the inner branches. Therefore, the postoperative cases have computational meshes with more elements, leading to higher computational costs.
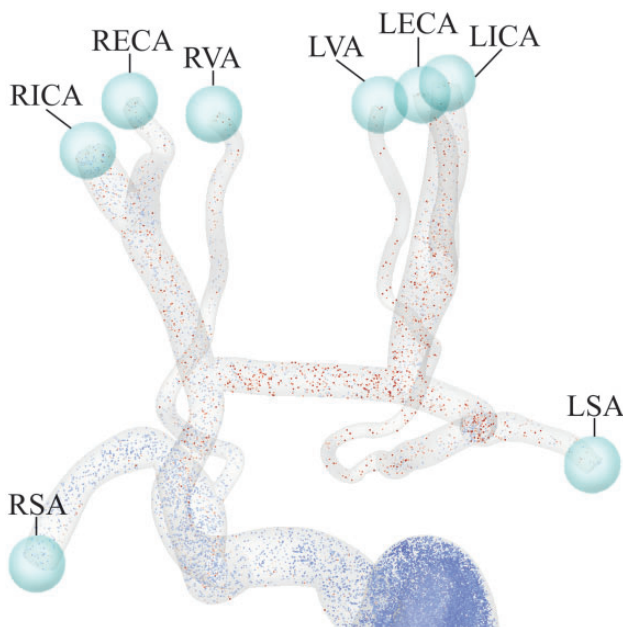
Figure 3: Representation of the virtual spheres used to capture particles leaving the domain through each vessel, enabling calculation of average platelet activation potential values for each of the supra-aortic arteries. LECA: left external carotid artery; LICA: left internal carotid artery; LSA: left subclavian artery; LVA: left vertebral artery; RECA: right external carotid artery; RICA: right internal carotid artery; RSA: right subclavian artery; RVA: right vertebral artery.

hemisphere (RHS) was calculated as the sum of the flows through the right internal carotid artery, right external carotid artery and right vertebral artery. Similarly, blood flow to the left hemisphere (LHS) was calculated as the sum of the flows through left internal carotid artery, left external carotid artery and left vertebral artery. Total CBF was calculated as the sum of LHS and RHS flows.

Total CBF was reduced in all endovascular repair scenarios, and double branch scenarios performed better compared to single branch alternatives (CBF changes of -1.4% and -2.0% for Scenarios 1 and 2 vs -4.8% and -3.6% in Scenarios 3 and 4, respectively). Blood flow to the LHS decreased more compared to RHS flow in all repair scenarios. Again, scenarios with a double-branch endograft performed better compared to the single branch alternatives (LHS flow changes of -2.3% and -3.4% in Scenarios 1 and 2 vs -6.7% and -5.6% in Scenarios 3 and 4, respectively).

Impact of endograft design on blood shear rate

PLAP metrics were computed following injection and tracking of particles during 10 cardiac cycles. Average PLAP was calculated at the outflows of the cervical arteries. Significant differences in PLAP were revealed between the different endovascular repair scenarios. Table 3 summarizes the calculated mean PLAP values for all scenarios. Figure 5 presents a qualitative comparison of PLAP maps, showing colour-coded advected particles 2.4 s after virtual injection.

Mean PLAP was increased in all endovascular repair scenarios compared to the preoperative situation. Scenario 1 performed best with a mean PLAP increase of 14.7% in the cervical arteries. Scenario 3 performed the worst with an increase in the mean PLAP of 74.3%. The endograft used in Scenario 3 had a single retrograde inner branch, which caused all blood flowing to the supra-aortic arteries to make a U-turn in the aortic arch and pass through the single outlet, increasing blood shear rates.

DISCUSSION

Multiple manufacturers are developing branched endografts for Zone 0 deployment, enabling total endovascular repair of the
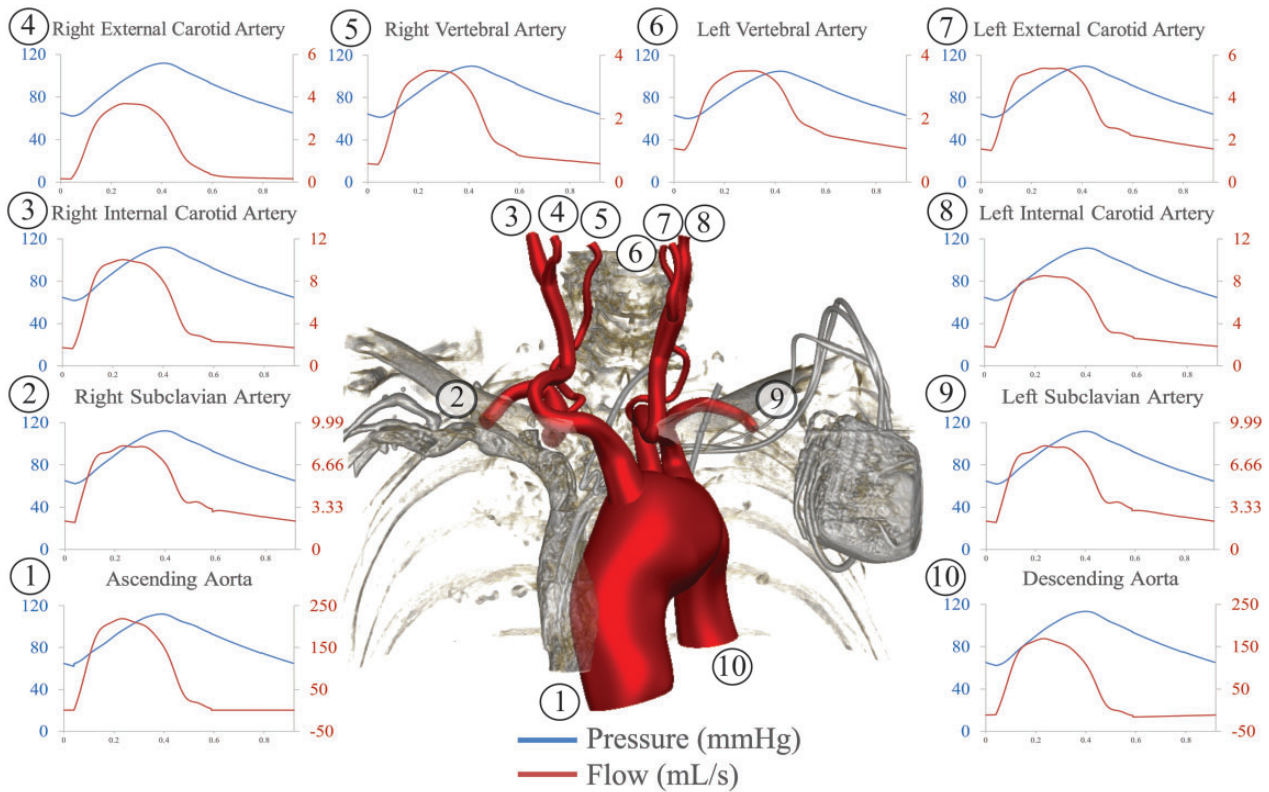
Figure 4: Top: pressure (blue lines) and flow (red lines) waveforms at the inlet (ascending aorta) and all outlets of the preoperative model. The location of each measurement is denoted by a number. Bottom: comparison between measured and computed blood flows and pressures in the preoperative model, with percentage differences between the 2 shown.

aortic arch. These devices extend the armamentarium for treatment of aortic arch pathologies, providing a solution for patients unfit for open surgical repair. The present study aimed to compare the postoperative haemodynamic performance of different endograft designs for Zone 0 endovascular aortic repair using advanced computational modelling analyses. This approach enables studying detailed haemodynamic indices without the need for performing invasive interventions in diseased patients. Furthermore, it facilitates virtual testing of different treatment scenarios in the same patient in a controlled setting. Haemodynamic performance was quantified for the different endograft designs by calculating changes in total CBF and average blood shear rate in the cervical arteries.

The use of double branch endografts, with 2 antegrade inner branches, resulted in smaller reductions in CBF compared to single branched alternatives (-1.4% and -2.0% vs -4.8% and -3.6%, respectively). When differential changes in blood flow to the RHS and LHS were calculated, blood flow to the LHS experienced the largest reduction in all endovascular repair scenarios (up to -6.7% in Scenario 3). This finding underlines the need for assessment of the circle of Willis before performing total endovascular aortic arch repair, as normal anatomy with a complete circle is present in only 28% of the population [21]. Most frequent anatomical variations include hypoplasia of the posterior communicators (22%) and absence or hypoplasia of either the A1 segment of the anterior cerebral artery (25%) or the posterior communicator (15%) [22, 23].

Table 2: Simulated mean flow values

	Preoperative (mL/min)	Scenario 1 (mL/min)	Scenario 2 (mL/min)	Scenario 3 (mL/min)	Scenario 4 (mL/min)
Ascending aorta	4665	4665	4665	4665	4665
Right subclavian artery	283	280	280	282	286
Right external carotid artery	90	90	90	87	88
Right internal carotid artery	296	294	295	287	290
Right vertebral artery	104	103	104	104	105
Left vertebral artery	126	120	119	117	118
Left internal carotid artery	272	269	266	255	258
Left external carotid artery	192	188	186	179	181
Left subclavian artery	284	273	270	264	267
Descending aorta	3019	3053	3059	3093	3072
Mean flow to RHS	490	488 (−0.4%)	488 (−0.3%)	477 (−2.5%)	483 (−1.3%)
Mean flow to LHS	591	577 (−2.3%)	570 (−3.4%)	551 (−6.7%)	558 (−5.6%)
Total mean CBF	1080	1065 (−1.4%)	1059 (−2.0%)	1029 (−4.8%)	1041 (−3.6%)

CBF: cervical blood flow; LHS: left hemisphere; RHS: right hemisphere.

Table 3: Calculated mean PLAP values at the outflow branches

	Preoperative	Scenario 1	Scenario 2	Scenario 3	Scenario 4
Right subclavian artery	106.42	109.67	120.08	164.08	125.43
Right external carotid artery	129.66	132.22	129.05	200.53	181.34
Right internal carotid artery	119.53	105.49	110.57	188.82	162.98
Right vertebral artery	173.87	182.98	192.51	238.05	201.29
Left vertebral artery	218.15	340.34	388.18	427.16	361.87
Left internal carotid artery	127.89	135.04	170.37	261.69	214.74
Left external carotid artery	141.37	147.89	183.29	270.89	230.30
Left subclavian artery	108.31	153.45	202.50	263.17	219.48
Descending aorta	78.80	60.13	70.06	67.86	61.15
Mean PLAP cervical arteries	151.75	173.99 (+14.7%)	195.66 (+28.9%)	264.52 (+74.3%)	225.42 (+48.6%)

PLAP: platelet activation potential.

This is valuable information when planning Zone 0 endovascular repair, as patients with incomplete circles cannot compensate for a reduction in blood flow to the LHS through redistribution [21]. Reductions in cerebral blood flow could hypothetically be compensated through cerebral autoregulation; nonetheless, this would be the same for all endograft designs. In addition, the target population for these endografts is diseased patients, in whom reserve capacity for cerebral autoregulation will likely be impaired [24, 25].

The alterations in blood shear rate were calculated using the so-called PLAP index, which has been related to thrombus formation in aortic flows previously [8, 20]. Both single branch endografts resulted in larger increments in blood shear rates in the cervical arteries compared to the double branch devices (74.3% and 48.6% increase vs 14.7% and 28.9% increase, respectively). The increases in blood shear rate are inherent and mostly unavoidable consequences of the altered morphology of the aorta and supra-aortic arteries following Zone 0 repair.

Reduced perfusion, in combination with increased blood shear rates may have negative long-term consequences, particularly in the cerebral microcirculation. Evidence from epidemiological, clinical and experimental studies indicates that cerebral hypoperfusion and microcirculatory dysfunction play a critical role in the pathogenesis of many types of vascular cognitive impairment and dementia, including Alzheimer's disease [25–27].

We hypothesized that Zone 0 endograft design has a significant impact on the postoperative haemodynamic performance, particularly in the cervical arteries. Our results confirm this hypothesis. In the present study, double branch endografts offered better postoperative haemodynamic performance compared to single branch alternatives. We believe that the closer an endograft design is to preserving preoperative aortic morphology, the smaller the postoperative haemodynamic disturbances will be.

The advantages of a double branch design highlighted above focus on postoperative haemodynamic performance and may be offset during device deployment. Single branch devices could be easier to deploy, requiring less catheter manipulation in the aortic arch, which is considered to be the main risk factor for perioperative embolic stroke [6]. On the other hand, single branch devices require an additional extra-anatomical bypass, potentially increasing perioperative risks [4].

Limitations

The patient who is presented in this study was not treated with any of the studied endografts, making it impossible to relate our computational predictions to *in vivo* follow-up data. Furthermore, performing the same 'virtual testing' analysis in
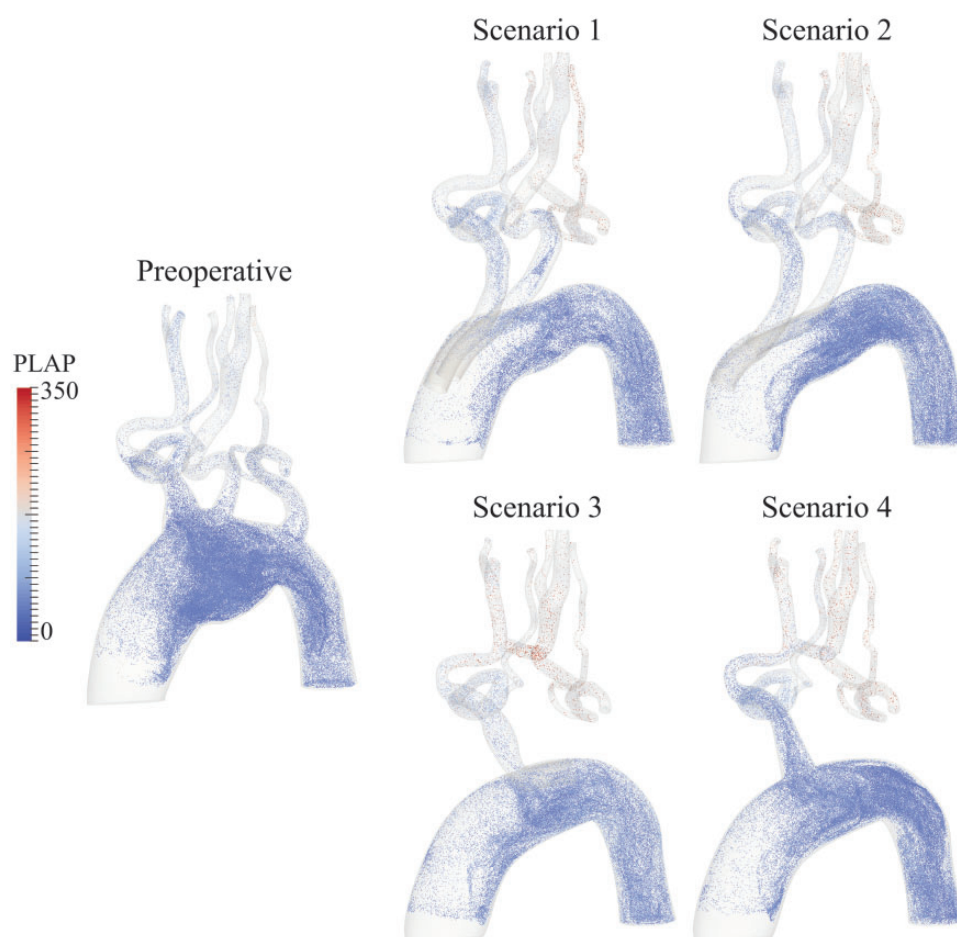
Figure 5: The image visualizes the position and PLAP values, representing the amount of accumulated blood shear rate, of particles 2.4 s after virtual injection at the ascending aorta for all scenarios. All postoperative scenarios show elevated values of shear rate in the supra-aortic arteries compared to the preoperative situation. Furthermore, Scenarios 3 and 4 present higher values of blood shear rate in the cervical arteries compared to Scenarios 1 and 2. PLAP: platelet activation potential.

patients with different anatomical features could potentially lead to different postoperative results. However, as the differences in aortic arch anatomy between patients are relatively small compared to the differences between the endograft designs and resulting postoperative morphology, we can say from our experience that the likelihood of obtaining drastically different results among patients is small.

When considering the value of 'population-based' analyses, it is important to realize the fundamental differences between these and 'patient-specific' analyses. In 'population-based' studies, few aspects of the system are known or controlled, and therefore, many subjects are needed to extract conclusions. In computational modelling, a 'patient-specific' paradigm produces highly detailed results for 1 specific patient, which can be used to identify optimal devices or interventions for that specific patient [10]. The value of this article is to offer a controlled, 'apples-to-apples' comparison between different device designs for the same patient, and as such, we are confident that our results are sound, given the extensive validation work done in our code.

All postoperative scenarios were run with equal boundary conditions relative to the preoperative model, meaning that the cardiac output and outflow boundary conditions (i.e. Windkessel parameters) did not change after endovascular intervention and between the different scenarios. These assumptions enable fair comparison of haemodynamics between the endovascular repair

scenarios, but their validity has not been determined yet. The endograft alters the postoperative left ventricular afterload due to the much higher stiffness relative to the native aorta, potentially affecting cardiac performance [28]. Additionally, the reduced number of postoperative supra-aortic outflow tracts may also contribute to an increase in left ventricular afterload relative to the preoperative conditions. Furthermore, it has been reported previously that devices or catheters inserted in the aorta lead to increases in left ventricular afterload and ultimately to changes in cardiac performance [29]. In addition, following endovascular repair, patients are often prescribed antihypertensive medications, which affect the vascular resistance and may alter cardiac output chronically.

The computations in this work have been carried out assuming a rigid behaviour for the arterial wall. Simulating the interactions between blood flow and vessel wall motion is possible [30], but it would increase computational cost significantly without altering the observed differences in haemodynamics between the different endograft designs. Of note, all computed flow and pressure values lay within 5% of the clinical data in the preoperative simulation.

CONCLUSIONS

Double branch Zone 0 endograft designs offer superior postoperative haemodynamic performance compared to single branch

alternatives for total endovascular aortic arch repair, minimizing reductions in CBF and alterations in blood shear rate that could potentially lead to cerebral ischaemic events. Reductions in CBF might be particularly problematic in patients with an incomplete circle of Willis, where reductions in blood flow to the LHS cannot be compensated through redistribution.

CFD provides a powerful tool to enhance our understanding of haemodynamics in complex aortic anatomies and optimize the design and planning of advanced endovascular procedures.

SUPPLEMENTARY MATERIAL

Supplementary material is available at *EJCTS* online.

Conflict of interest: Kim A. Eagle received grants from W.L. Gore and Medtronic Inc. during the course of this study. Himanshu J. Patel serves as consultant and co-patent holder with W.L. Gore and consultant for Medtronic Inc. Santi Trimarchi serves as consultant and speaker for W.L. Gore and Medtronic Inc. Joost A. van Herwaarden serves as consultant and speaker for Bolton Medical, Cook Medical and Philips Health Care. All authors declare no conflict of interest related to the content of the manuscript.

REFERENCES

[1] Patel HJ, Deeb MG. Ascending and arch aorta pathology, natural history, and treatment. Circulation 2008;118:188–95.

[2] Lioupis C, Abraham CZ. Results and challenges for the endovascular repair of aortic arch aneurysms. Perspect Vasc Surg Endovasc Ther 2011; 23:202–13.

[3] Anthony Lee W. Status of branched grafts for thoracic aortic arch endovascular repair. Semin Vasc Surg 2016;29:84–9.

[4] Andrasi TB, Grossmann M, Zenker D, Danner BC, Schondube FA. Supra-aortic interventions for endovascular exclusion of the entire aortic arch. J Vasc Surg 2017;66:281–97.e2.

[5] Spear R, Haulon S, Ohki T, Tsilimparis N, Kanaoka Y, Milne CPE *et al*. Editor's Choice—subsequent results for arch aneurysm repair with inner branched endografts. Eur J Vasc Endovasc Surg 2016;51:380–5.

[6] Ullery BW, McGarvey M, Cheung AT, Fairman RM, Jackson BM, Woo EY *et al*. Vascular distribution of stroke and its relationship to perioperative mortality and neurologic outcome after thoracic endovascular aortic repair. J Vasc Surg 2012;56:1510–17.

[7] Melissano G, Tshomba Y, Bertoglio L, Rinaldi E, Chiesa R. Analysis of stroke after TEVAR involving the aortic arch. Eur J Vasc Endovasc Surg 2012;43:269–75.

[8] Nauta FJ, Lau KD, Arthurs CJ, Eagle KA, Williams DM, Trimarchi S *et al*. Computational fluid dynamics and aortic thrombus formation following

[9] Arthurs CJ, Agarwal P, John AV, Dorfman AL, Grifka RG, Figueroa CA. Reproducing patient-specific hemodynamics in the Blalock–Taussig circulation using a flexible multi-domain simulation framework: applications for optimal shunt design. Front Pediatr 2017;5:78.

[10] van Bakel TMJ, Lau KD, Hirsch-Romano J, Trimarchi S, Dorfman AL, Figueroa CA. Patient-specific modeling of hemodynamics: supporting surgical planning in a Fontan circulation correction. J Cardiovasc Transl Res 2018; doi:10.1007/s12265-017-9781-x.

[11] Fagard R, Conway J. Measurement of cardiac output: Fick principle using catheterization. Eur Heart J 1990;11:1–5.

[12] Taylor CA, Figueroa CA. Patient-specific modeling of cardiovascular mechanics. Annu Rev Biomed Eng 2009;11:109–34.

[13] CRIMSON. The Software for Cardiovascular Modelling and Simulation. www.crimson.software (13 February 2018, date last accessed).

[14] Sahni O, Müller J, Jansen KE, Shephard MS, Taylor CA. Efficient anisotropic adaptive discretization of the cardiovascular system. Comput Methods Appl Mech Eng 2006;195:5634–55.

[15] Westerhof N, Lankhaar JW, Westerhof BE. The arterial Windkessel. Med Biol Eng Comput 2009;47:131–41.

[16] Lantz BMT, Foerster JM, Link DP, Holcroft JW. Regional distribution of cardiac output: normal values in man determined by video dilution technique. Am J Roentgenol 1981;137:903–7.

[17] Nobili M, Sheriff J, Morbiducci U, Redaelli A, Bluestein D. Platelet activation due to hemodynamic shear stresses: damage accumulation model and comparison to in vitro measurements. ASAIO J 2008;54:64–72.

[18] Shankaran H, Alexandridis P, Neelamegham S. Aspects of hydrodynamic shear regulating shear-induced platelet activation and self-association of von Willebrand factor in suspension. Blood 2003;101:2637–45.

[19] Shadden SC, Hendabadi S. Potential fluid mechanic pathways of platelet activation. Biomech Model Mechanobiol 2013;12:467–74.

[20] Di Achille P, Tellides G, Figueroa CA, Humphrey JD. A haemodynamic predictor of intraluminal thrombus formation in abdominal aortic aneurysms. Proc R Soc A Math Phys Eng Sci 2014;470:20140163.

[21] Karatas A, Coban G, Cinar C, Oran I, Uz A. Assessment of the circle of Willis with cranial tomography angiography. Med Sci Monit 2015;21: 2647–52.

[22] Riggs H, Rupp C. Variation in form of circle of Willis. The relation of the variations to collateral circulation: anatomic analysis. Arch Neurol 1963; 8:8–30.

[23] Fabian TC. Blunt cerebrovascular injuries: anatomic and pathologic heterogeneity create management enigmas. J Am Coll Surg 2013;216: 873–85.

[24] Roy B, Woo MA, Wang DJJ, Fonarow GC, Harper RM, Kumar R. Reduced regional cerebral blood flow in patients with heart failure. Eur J Heart Fail 2017; doi:10.1002/ejhf.874.

[25] Toth P, Tarantini S, Csiszar A, Ungvari Z. Functional vascular contributions to cognitive impairment and dementia: mechanisms and consequences of cerebral autoregulatory dysfunction, endothelial impairment, and neurovascular uncoupling in aging. Am J Physiol Heart Circ Physiol 2017;312:H1–20.

[26] Kim HA, Miller AA, Drummond GR, Thrift AG, Arumugam TV, Phan TG *et al*. Vascular cognitive impairment and Alzheimer's disease: role of cerebral hypoperfusion and oxidative stress. Naunyn Schmiedebergs Arch Pharmacol 2012;385:953–9.

[27] Duncombe J, Kitamura A, Hase Y, Ihara M, Kalaria RN, Horsburgh K. Chronic cerebral hypoperfusion: a key mechanism leading to vascular cognitive impairment and dementia. Closing the translational gap between rodent models and human vascular cognitive impairment and dementia. Clin Sci 2017;131:2451–68.

[28] Nauta FJH, Kamman AV, Ibrahim E-SH, Agarwal PP, Yang B, Kim K *et al*. Assessment of CardiOvascular Remodelling following Endovascular aortic repair through imaging and computation: the CORE prospective observational cohort study protocol. BMJ Open 2016;6:e012270.

[29] Cuomo F, Ferruzzi J, Humphrey JD, Figueroa CA. An experimental-computational study of catheter induced alterations in pulse wave velocity in anesthetized mice. Ann Biomed Eng 2015;43:1555–70.

[30] Figueroa CA, Vignon-Clementel IE, Jansen KE, Hughes TJR, Taylor CA. A coupled momentum method for modeling blood flow in three-dimensional deformable arteries. Comput Methods Appl Mech Eng 2006;195:5685–706.

thoracic endovascular aortic repair. Ann Thorac Surg 2017; doi: 10.1016/j.athoracsur.2016.09.067.